Available online www.ejaet.com

European Journal of Advances in Engineering and Technology, 2020, 7(12):32-38

Research Article ISSN: 2394 - 658X

Structural, Thermal, & Dielectric Study of Lanthanum/Yttrium/ Magnesium Nanoferrites

Sumaira Nosheen[1,2], Sadia Sagar Iqbal[1], Phool Shahzadi[2], Aneela Sabir[1], Rafiullah Khan[1] and Tasawar Shahzad[3]

[1]Department of Polymer Engineering and Technology, University of the Punjab, Pakistan
[2]PCSIR Laboratories Complex Ferozepur Road Lahore, Pakistan
[3]Department of Physics, University of Lahore
Sumera_pcsir@yahoo.com

ABSTRACT

La+3 substituted spinel ferrites with composition $LaxMg_{0.8-xY0.2}Fe_2O_4$ where values of x are 0, 0.15, 0.35, 0.55, 0.7 plus 0.8 were fabricated by following sol-gel auto combustion process. Nitrates were employed as preliminary chemicals. 600oC is stable phase of formulated nanoferrites which was confirmed by TGA. Structural interpretation of all synthesized nanoferrites specimens was carried out by means of XRD, SEM in addition to FTIR process. Fabricated ferrite x-ray pattern confirms cubic spinel ferrite configuration. La+3 replacement effect on diverse fundamental criterion of yttrium magnesium ferrites was perceived. Dielectric properties for instance dielectric constant, dielectric loss along with ac conductivity as a part of frequency on room temperature goes on mounting with incorporation of Lanthanum ion in Yttrium Magnesium nanoferrites.

Key words: La-Y-Mg ferrite, IR study, Electric, Thermal

INTRODUCTION

In the old age, lodestones were used for direction purpose. Mankind has used different types of magnetic materials for their common applications. The actual use of the magnetic materials was began to understand after the invention of electricity. It is now recognized that lodestone is an iron ore called magnetite, which is one of the wide ranges of magnetic ceramics based on iron (III)oxide, called the ferrites [1]. Generally, the physical properties of ferrite materials are governed by processing techniques, stoichiometry, and also the dispersion of cations among tetrahedral-A sites and octahedral-B sites. The preference of cation to occupy either A, or B sites are dependent on their ionic radius, crystal field, electronic configuration and also the ionic polarization [2-5]. Recently, spinel nanoferrites have been used in numerous technological and scientific applications [6-10]. The spinel ferrites are classified into three types such as normal spinel structure, inverse spinel structure, and intermediate spinel structure. In normal spinel ferrites, divalent ions are at tetrahedral A-site and trivalent ions are in octahedral B-site; in inverse spinel structure, half of the trivalent ions are at B-site and half at A-site and the remaining ions are distributed in octahedral B-site, whereas intermediate spinel structure possesses the intermediate stage between the normal and inverse spinel ferrites [11].

Here numerous attempts have been made in order to enhance the qualities of ferrites by incorporating the same suitable nonmagnetic/diamagnetic impurities with different valence state at the A and B sites includes Copper [12,13], Manganese [14], Praseodymium [15], Lanthanum [16], Neodimium [17] ion and etc [18]. Lanthanum is known as the second most abundant and lightest rare earth element (REE) in the lanthanide series. This silvery white mineral found in monazite and bastnasite ores. Lanthanum possesses distinct quality as compared to other REE such as simple electronic spectra which is helpful for experimental analysis; it has the highest boiling point and lowest vapor pressure at its melting point; and at atmospheric pressure lanthanum is the only superconducting REE [19]. Therefore, lanthanum is demand for some important application includes a) used in the manufacture of expensive glasses as lanthanum imparts a high refractive index to the glass [20]) used in NiMH batteries that are currently used in almost all hybrid-electric vehicles [21,22] Lanthanum rich compounds are used in alloy and fluid cracking catalyst for petroleum refinery

industry [23]. Rare earth materials are known to possess good electrical insulation properties with high electrical resistivity. Therefore, the substitution of these rare earth ions into spinel ferrites could alter the electrical and magnetic properties. Moreover, these rare earth ions have a huge influence on the magnetic anisotropy of the system making the spinel ferrite as promising materials replacing the hexaferrite or garnets [15, 23].

Various methods have been employed in order to synthesize the soft spinel ferrite materials Including chemical co-precipitation [24], hydrothermal method [25], mechano-chemical method [26], microemulsion method [24], rheological phase reaction method [27], and also sol-gel method [28]. Wu et al. [28] synthesized Ni 0.5Zn 0.5LaxFe$_2$–xO$_4$ using solid-state reaction at low temperatures for the first time. The results showed that the calcination temperature affects the magnetic properties of lanthanum substituted Ni-Zn ferrite, while the highest coercivity value of 120.09 O^e obtained at 800°C of calcination temperature. Ahmed et al. [30] have examined the structural and electrical properties of La3+ substituted Ni-Zn ferrite prepared by standard ceramic method. Among these techniques, sol-gel synthesis has been receiving much attention as they can be applied to an extremely wide variety of materials and also they offer the possibility of controlling the size, shape, and distribution of particles [29].

There aren't many research works focused on the detailed structural and morphological analysis of the lanthanum ion substitution into the spinel ferrite materials. Therefore, the current work is intended on investigating the effect of rare earth lanthanum ion substitution and distribution within the A and B sublattices on the structural, magnetic (super exchange interactions and spin alignment) and morphological properties of Ni-Zn ferrite nanoparticles.

Though, no description in literature is found for La+3 substituted Y-Mg ferrites formulated by sol gel auto-combustion process. Within this statement, we describe La+3 replacement consequence on fundamental characteristics of yttrium magnesium nano spinel ferrites formulated via sol gel technique.

EXPERIMENTAL

Formation of $La_xMg_{0.8-x}Y_{0.2}Fe_2O_4$ (x= 0, 0.15, 0.35, 0.55, 0.7 and 0.8) ferrite

Nano-ferrite structure having composition LaxMg$_{0.8-x}$Y$_{0.2}$Fe$_2$O$_4$ (x = 0, 0.15, 0.35, 0.55, 0.7 and 0.8) was formulated via sol gel auto-combustion process. AR grade higher transparency yttrium, lanthanum, magnesium plus ferrous nitrate utilized as preliminary reagents. The entire chemicals measured in required amount on weighing balance. For 10g of product lanthanum, magnesium, yttrium and iron nitrate salts were mixed in 100ml ethanol using constant stirring with heating on 50 °C. Subsequently after half an hour added 20ml 3M NH_3 solution in metal precursor mixture and increased temperature up to 100 °C. Later in this solution, added 1ml PEG, stirring (7rpm) and temperature (220 °C) increased then further added 10 ml NH_3 solution. After 30-35 min. stop stirring and increased temperature up to 235 °C, after a short time in sample auto-combustion will take place which converts gel into powder form. Obtained powder is finely grinded, then sintered inside electric furnace on temperature lower than melting point of constituent elements.

RESULTS AND DISCUSSION

Morphological Study

Scanning Electron Microscope

Micrographs of scanning electron microscopy of formulated nanoferrites illustrated by Figure 1. Nano-size particles aggregation in shape of micron size grains shown by Micro-images. In micrographs response of lanthanum doping is noticeably recognized. Figure-1a represents yttrium magnesium ferrite nanoparticles are spherical formed of about 30 μm in size having extremely uneven surface. However subsequent to lanthanum addition, particles size starts decreasing upto 5 μm in average also the surface turn out plane as in Fig. 1 (b, c, d, e, f) in contrast with Figure 1a. The cause belong to this manners is the consequence on crystallization response of yttrium magnesium nanoferrites which cause the creation of octahedral form with even surface of nanoparticles. The rising forces involving Van-der walls, capillary as well as electrostatic forces participated to enhance the mutual interaction among particles with elevated calcination temperature.

X-ray diffraction

Formulated $Y_{0.2}La_XMg_{0.8-X}$ Fe_2O_4 (x = 0, 0.15, 0.35, 0.55, 0.7 and 0.8) nanoferrites XRD design are portrayed in Fig. 2. Single-phase cubic spinal structure is cleared from XRD graphs. The noticed XRD peaks are (111), (220), (311), (400), (422), (511) and (440) planes illustrate the single-phase Y-Mg nanoferrites. Whereas, the peak correspondent at 2θ = 32.21° is (200) attributed to the secondary phase of Lanthanum ferrites at the grain boundaries with ICDD card # 74–2203. The intensity of $LaFeO_3$ peak is enhanced with the increase concentration of La^{3+} ion furthermore secondary phase of Fe_2O_3 at 2θ = 33.22° with card number 86–2368 is noticed with increase concentration of lanthanum ion**.**

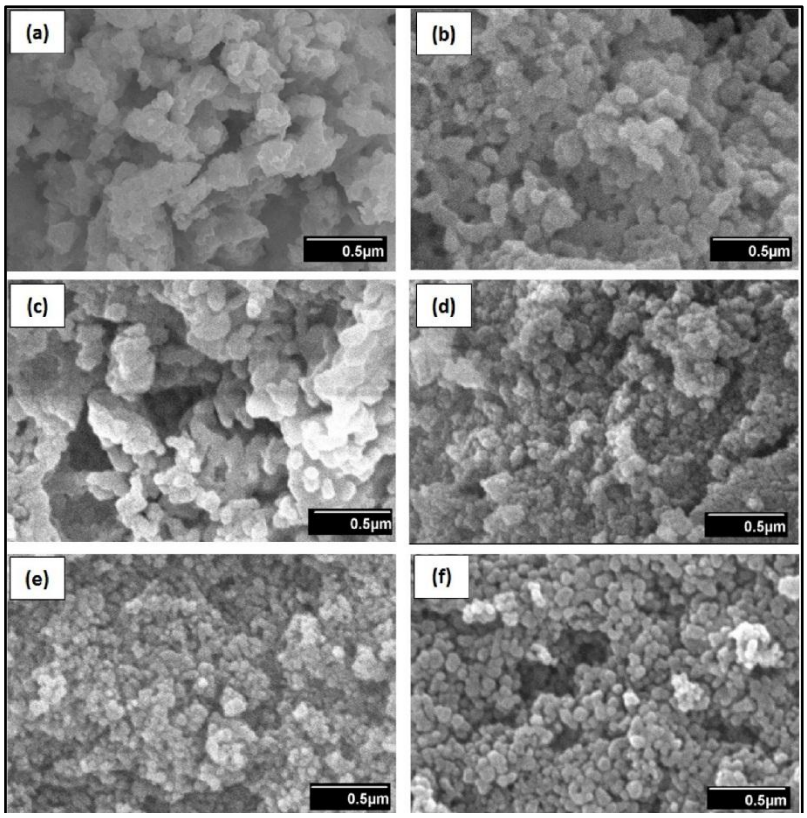

Fig. 1 Synthesized lanthanum doped yttrium magnesium ferrites $Y_{0.2}La_XMg_{0.8-X}Fe_2O_4$ SEM micrographs (a) $Y_{0.2}Mg_{0.8}Fe_2O_4$,(b) $Y_{0.2}La_{0.15}Mg_{0.65}Fe_2O_4$,(c) $Y_{0.2}La_{0.35}Mg_{0.45}Fe_2O_4$, (d) $Y_{0.2}La_{0.55}Mg_{0.25}Fe_2O_4$, and (e) $Y_{0.2}La_{0.7}Mg_{0.1}Fe_2O_4$(f) $Y_{0.2}La_{0.8}Fe_2O_4$

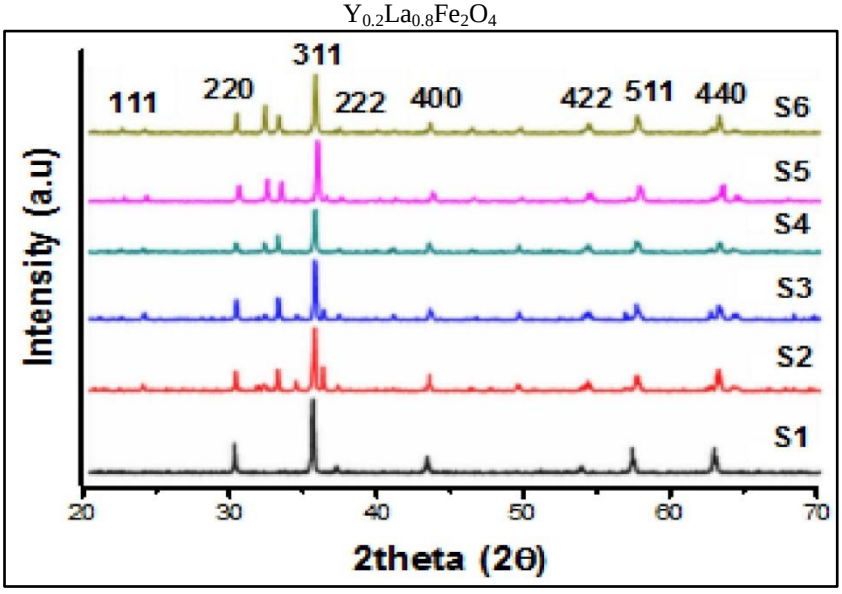

Fig. 2 Designed nanoferrites XRD pattern

FTIR Study of La-Y-Mg ferrite

An additional device employed to verify the creation of ferrites is FTIR. Waldron proposed the existence of most intense absorption bands as a result of tetrahedral as well as octahedral systems analogous to wave numbers on around $600cm^{-1}$ plus $400cm^{-1}$. Upper wave number assimilation cord is owing to fundamental metal oxygen stretching oscillation at tetrahedral positions (Mtetra ↔ O) as well as inferior wave number assimilation ring is owing to stretching at octahedral position (Mocta ↔ O). In case of spinel ferrites, it is recommended that 4 infra-red energetic bands, represented like ν1, ν2, ν3, ν4 with descending wave numbers**.** In regular and inverse spinel configuration, presence of these four bands streamlined on origin of set hypothetical measurements using space groups in addition to point conformity. It was well suggested that 4 bands amongst first three bands are essential, because of tetrahedral as well as octahedral systems, while

fourth band is as a result of different kinds of lattice oscillations. FTIR absorption spectra for investigated $Y_{0.2}La_XMg_{0.8-X}Fe_2O_4$ nanoferrites with enlarge doping of La^{3+} concentration are depicted in Fig. 3.

The regular and inverse cubic spinel ferrites configuration is clearly monitored the two basic absorption bands. The absorption band in 500-600 cm^{-1} range, generally signifies the tetrahedral group vibration, and in 350–490 cm^{-1} range absorption band represents the octahedral groups. At 572 cm^{-1} intrinsic band contribute to M↔O stretching oscillation of iron ion. For time being, at 1638 cm^{-1} corresponds to NO_3^{-1} ions as well as the presence of carboxyl group. The hydrogen bonded O-H stretching vibrations emerge at 3440 cm^{-1} as broad band appearance.

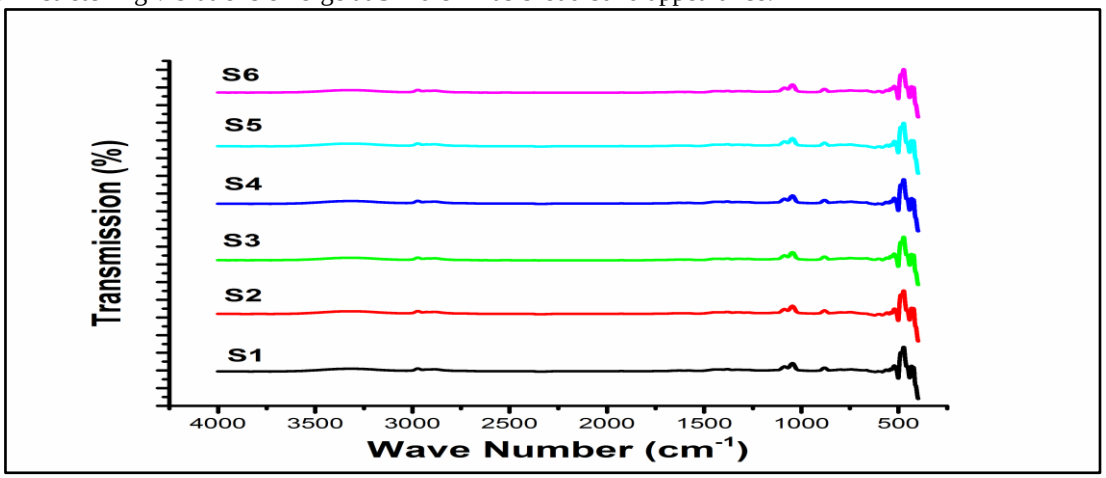

Fig. 3 Designed nanoferrites FTIR Spectra

Thermal Properties

Thermogravimetry Analysis (TGA)

In Figure-4 Yttirum magnesium nanoferrites thermograms are represented. By means of sol-gel process synthesized nanoferrites is investigated from room temperature to 1000 ^oC in oxygen atmosphere. In the first step, loss of moisture in the nano powder is noticed in the range of room temperature to 150 ^oC. At 400 ^oC at the closing stages of second step, the ignition of nitrates and the remaining carbon-based bodies are occurred. Additionally, no further mass loss is examined subsequent to this step. However, the S6 illustrate extra thermal stability than the other nanoferrites owing to the increased doping effect of the lanthanum ion.

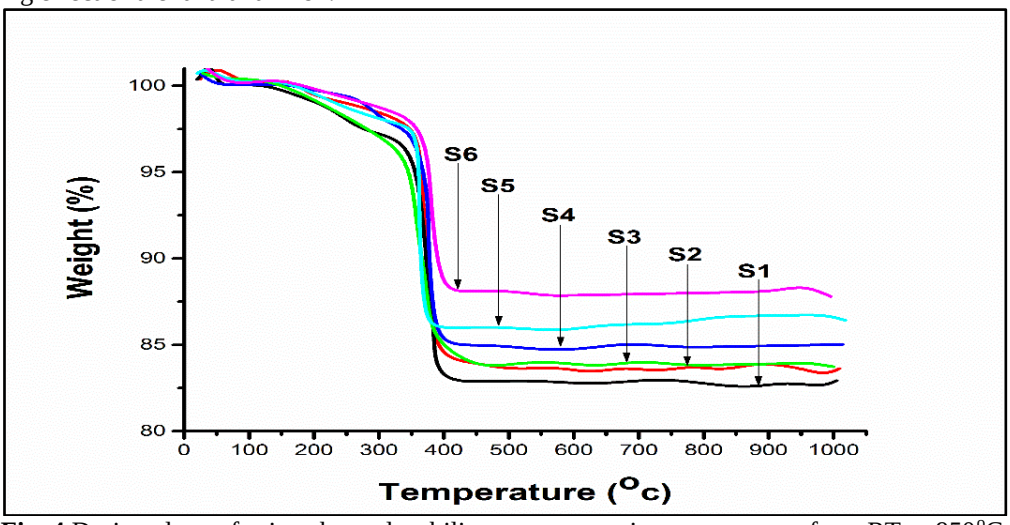

Fig. 4 Designed nanoferrites thermal stability response against temperature from RT to 950^oC

Differential Thermal analysis

Fabricated nano-ferrite samplesdifferential thermal analysis is carry out at 25-950 ^oC temperature condition in oxygen atmosphere and the collected proof is presented in Fig. 5. DTA thermo contours clarify an exothermic behavior in temperature range of 100-300 ^oC on account of evaporation/exhaust of hot gases. Additionally, endothermic series is evolved follow by scoop out heat which is engrossed by altering phases of nanoferrites. This affirms that nanoferrites are extremely dense with less porosity.

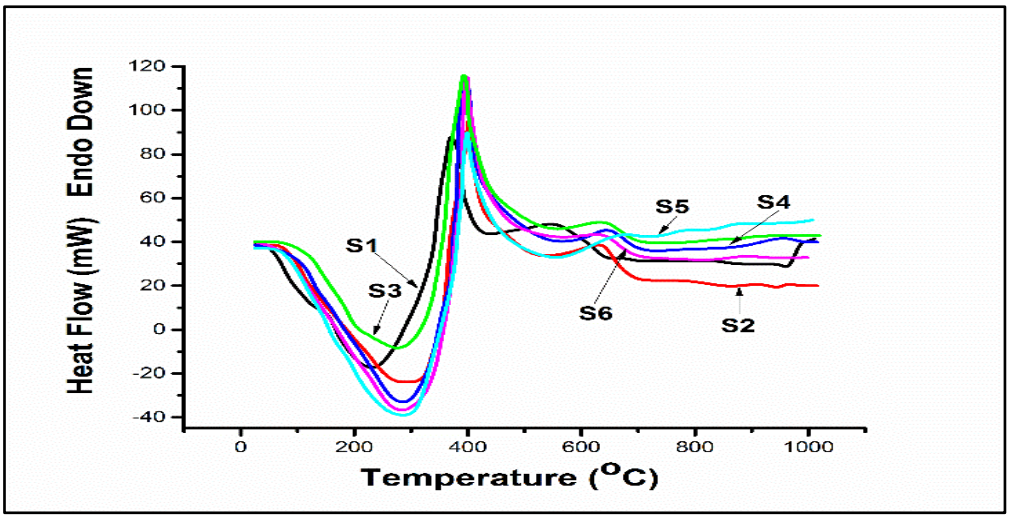

Fig. 5 Designed nanoferrites heat flow response against temperature from RT-950°C

Conductivity Study

Dielectric response

By considering examined materials two main properties, that is dielectric constant (ε') and loss factor the dielectric behavior can be described. Dielectric constants of the entire formulated nanoferrites are depicted in Fig. 6. From fig. 6, it is cleared that as a result of the conventional dielectric relaxation process, dielectric constant decreases as the frequency increases. Dielectric constant is steady with frequency varying in rising order. With addition of La ions the actual part of the dielectric properties increases, dielectric constant is increased three times when x = 0.8 reaches than when x = 0.0. Because interruption in iron ion bond length in octahedral site enhancing the polarization capacity owing to the doping effect of La ion. So, in the doped nanoferrites the dielectric constants are higher. As apparent from the Figure 6 that the dielectric constant decreases in the complete frequency range. Among ferric and ferries ions hopping of electrons is involved, when electric field is used and electrons are aligned as well as polarized. The hopping of electron is continuous with the increase frequency, which decreases the polarization due to the exchange of $Fe^{2+} \leftrightarrow Fe^{3+}$ ions is stopped.

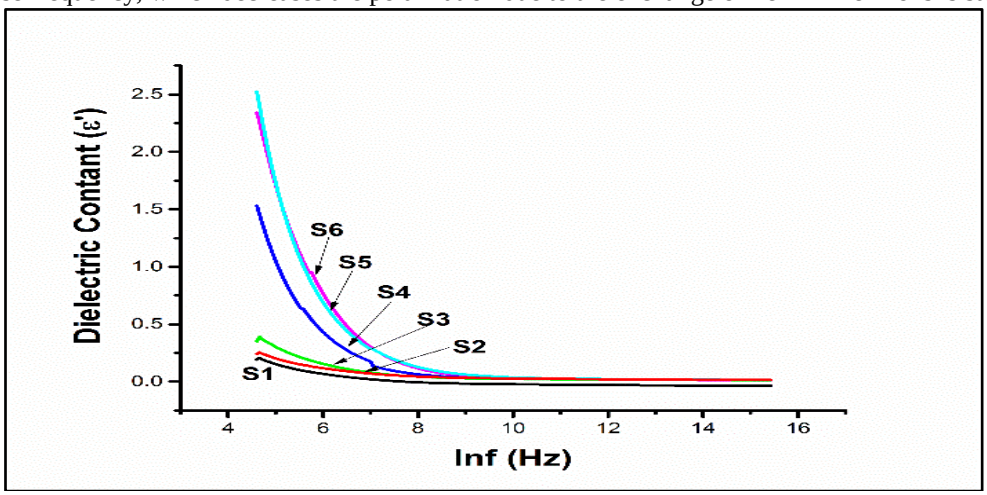

Fig. 6 Nanoferrites dielectric constant Vs lnf contours

Dielectric Loss

Dielectric loss factor is generally recognized as tangent delta which decreases with the increase of frequency as well as doping effect of La ion in yttrium magnesium nano-ferrites. tan δ increases with the increase of frequencies owing to interfacial polarization.

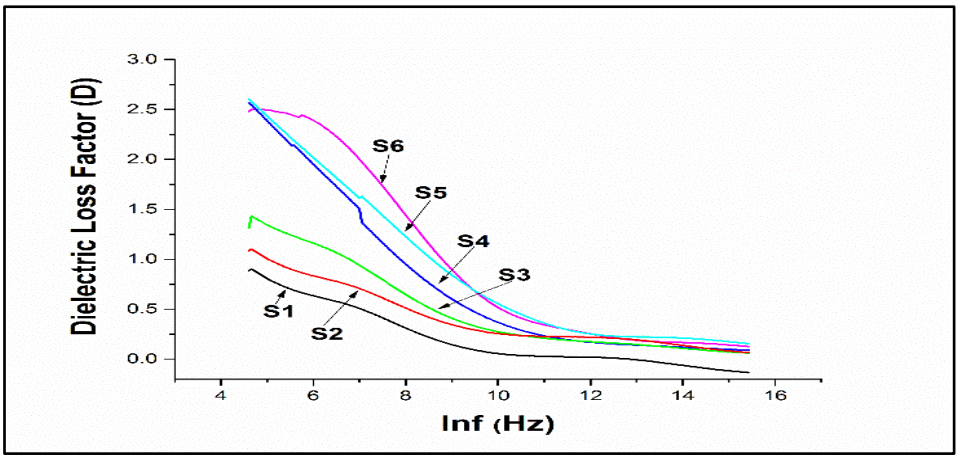

Fig. 7 Nanoferrites dielectric loss factor Vs Lnf contours

Ac conductivity

Yttrium magnesium nanoferrites ac conductivity is small than the La ion doped yttrium magnesium nanoferrites. Doped ferrites ac conductivity is higher owing to bouncing of electron at the grain boundaries on account of heterogeneities. But ac conductivity is steady with the increase of frequency due to the fewer jumping of electrons of iron ions in the octahedral positions.

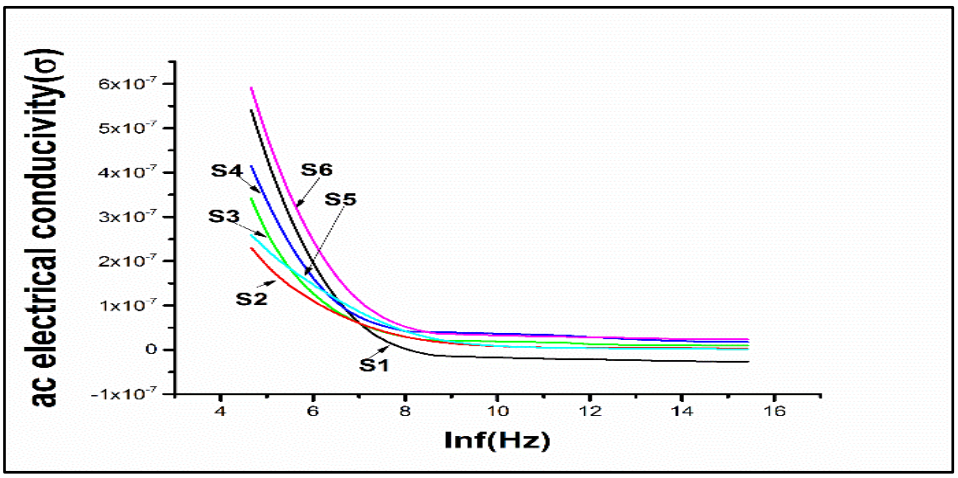

Fig. 8 Nanoferrites samples (x= 0, 0.15, 0.35, 6 0.55, 0.7, 0.8) Ac Conductivity Vs lnfContours

CONCLUSION

LaxMg0.8-xY0.2Fe2O4 (0 < x <0.8) nanoparticles series are proficiently formulated via sol-gel method. XRD, FTIR, and SEM are performed to verify the composition of nanoferrites. XRD investigation announces the creation of spheroidal shaped nanoparticles and cubic spinel structure of the ferrites. SEM micrographs furthermore confirmed the shape. And successful interfacial modification of La ion in position of Mg ion on yttrium nanoferrites system. Along TGA/DTA examination revealed that the thermal stability is improved with the doping of La ion in Mg-Y nanoferrites. Conductive measurements also support the pervious result that the doping increased the dielectric properties of nanoferrites.

Acknowledgements

An (unnumbered) acknowledgements section may be inserted if required. Information concerning research grant support and the assistance of colleagues or similar notes of appreciation may appear in Acknowledgements section at the end of the paper.

REFERENCES

[1]. Rezlescu, N. and Rezlescu, E., 1974. Dielectric properties of copper containing ferrites. *physica status solidi (a)*, *23*(2), pp.575-582.].

[2]. Najmoddin N, Beitollahi A, Kavas H, Mohseni SM, Rezaie H, Åkerman J, et al. XRD cation distribution and magnetic properties of mesoporous Zn-substituted $CuFe_2O_4$. Ceramics International. 2014;40(2):3619–25.

[3]. Ahmad I, Abbas T, Islam M, Maqsood A. Study of cation distribution for Cu–Co nanoferrites synthesized by the sol–gel method. Ceramics International. 2013;39(6):6735–41.

[4]. Hussain A, Abbas T, Niazi SB. Preparation of $Ni_{1-x}Mn_xFe_2O_4$ ferrites by sol–gel method and study of their cation distribution. Ceramics International. 2013;39(2):1221–5.
[5]. Kavas H, Baykal A, Toprak MS, Köseoğlu Y, Sertkol M, Aktaş B. Cation distribution and magnetic properties of Zn doped $NiFe_2O_4$ nanoparticles synthesized by PEG-assisted hydrothermal route. Journal of Alloys and Compounds. 2009;479(1):49–55
[6]. R.S. Yadava, I. Kuritkaa, J. Vilcakovaa, J. Havlicab, L. Kalinab, P. Urbaneka, M. Machovskya, D. Skodaa, M. Masara, M. Holeka, Sonochemical synthesis of Gd 3+ doped $CoFe_2O_4$ spinel ferrite nanoparticlesand its physical properties. Ultrason. Sonochem. 40, 773–783 (2018)].
[7]. Kovalenko, R.S. Yadav, J. Pospisil, O. Zmeskal, D. Karashanova, P. Heinrichova, M. Vala, J. Havlica, M. Weiter, Towards improved efciency of bulk-heterojunction. Solar cells using various spinel ferrite magnetic nanoparticles. Org. Electron. 39, 118–126 (2016)
[8]. P.N. Anantharamaiah, P.A. Joy, Tuning of the magnetostrictive prop erties of cobalt ferrite by forced distribution of substituted divalent metal ions at diferent crystallographic sites. J. Appl. Phys. 121, 093904 (2017)
[9]. X. Lasheras, M. Insausti, I. Gil de Muro, E. Garaio, F. Plazaola, M. Moros, L. De, J.M. de la Matteis, L.L. Fuente, Chemical synthesis and magnetic properties of monodisperse nickel ferrite nanoparticles for biomedical applications. J. Phys. Chem. C 120(6), 3492–3500 (2016)].
[10]. L. Kumar, M. Kar, Efect of La3+ substitution on the structural and magneto crystalline anisotropy of nanocrystalline cobalt ferrite ($CoFe_2$-x$LaxO_4$). Ceram. Int. 438, 4771–4778 (2012)].
[11]. Ahmed TT, Rahman IZ, Rahman MA. Study on the properties of the copper substituted NiZn ferrites. Journal of Materials Processing Technology. 2004;153–154:797–803.
[12]. Sláma J, Grusková A, Ušáková M, Ušák E, Dosoudil R. Contribution to analysis of Cu-substituted NiZn ferrites. Journal of Magnetism and Magnetic Materials. 2009;321(19):3346–51.
[13]. Sattar AA, El-Sayed HM, El-Shokrofy KM, El-Tabey MM. Effect of manganese substitution on the magnetic properties of nickel-zinc ferrite. Journal of Materials Engineering and Performance. 2005;14(1):99–103.
[14]. Peng Z, Fu X, Ge H, Fu Z, Wang C, Qi L, et al. Effect of Pr^{3+} doping on magnetic and dielectric properties of Ni–Zn ferrites by "one-step synthesis". Journal of Magnetism and Magnetic Materials. 2011;323(20):2513–8.
[15]. Wang Y, Wu X, Zhang W, Chen W. Synthesis and electromagnetic properties of La-doped Ni–Zn ferrites. Journal of Magnetism and Magnetic Materials. 2016;398:90–5.
[16]. Shinde TJ, Gadkari AB, Vasambekar PN. Influence of Nd^{3+} substitution on structural, electrical and magnetic properties of nanocrystalline nickel ferrites. Journal of Alloys and Compounds. 2012;513:80–5.
[17]. Huq M, Saha D, Ahmed R, Mahmood Z. Ni-Cu-Zn Ferrite Research: A Brief Review. Journal of Scientific Research. 2013;5(2):215–34.
[18]. Krishnamurthy N, Gupta CK. Extractive Metallurgy of Rare Earths: CRC Press; 2004.
[19]. Schwartz M. Encyclopedia of Materials, Parts and Finishes, Second Edition: CRC Press; 2002.
[20]. Humphries M. Rare Earth Elements: The Global Supply Chain: DIANE Publishing Company; 2010.
[21]. Chu S. Critical Materials Strategy: DIANE Publishing Company; 2011.
[22]. Survey G. Minerals Yearbook, 2008, V. 1, Metals and Minerals: U.S. Government Printing Office; 2011.
[23]. Pervaiz E, Gul I, editors. Influence of rare earth (Gd^{3+}) on structural, gigahertz dielectric and magnetic studies of cobalt ferrite Journal of Physics: Conference Series; 2013: IOP Publishing.
[24]. Dar MA, Shah J, Siddiqui W, Kotnala R. Study of structure and magnetic properties of Ni–Zn ferrite nano-particles synthesized via co-precipitation and reverse micro-emulsion technique. Applied Nanoscience. 2014;4(6):675–82.
[25]. Köseoğlu Y, Bay M, Tan M, Baykal A, Sözeri H, Topkaya R, et al. Magnetic and dielectric properties of $Mn_{0.2}Ni_{0.8}Fe_2O_4$ nanoparticles synthesized by PEG-assisted hydrothermal method. Journal of Nanoparticle Research. 2011;13(5):2235–44.
[26]. Yang H, Zhang X, Ao W, Qiu G. Formation of $NiFe_2O_4$ nanoparticles by mechanochemical reaction. Materials Research Bulletin. 2004;39(6):833–7.
[27]. Jing J, Liangchao L, Feng X. Structural analysis and magnetic properties of Gd-doped Li-Ni ferrites prepared using rheological phase reaction method. Journal of Rare Earths. 2007;25(1):79–83.
[28]. Wu X, Wu W, Qin L, Wang K, Ou S, Zhou K, et al. Structure and magnetic properties evolution of nickel–zinc ferrite with lanthanum substitution. Journal of Magnetism and Magnetic Materials. 2015;379:232–8.
[29]. Valenzuela R. Magnetic ceramics: Cambridge University Press; 2005.
[30]. Ahmed M, Ateia E, Salah L, El-Gamal A. Structural and electrical studies on La^{3+} substituted Ni–Zn ferrites. Materials chemistry and physics. 2005;92(2):310–21.